

# Thermodynamic analysis of backpressure and condensing steam turbines from cogeneration system

Mrzljak Vedran<sup>1</sup>, Prpić-Oršić Jasna<sup>1</sup>, Poljak Igor<sup>2</sup>, Gospić Ivan<sup>2</sup>

<sup>1</sup>Faculty of Engineering, University of Rijeka, Vukovarska 58, 51000 Rijeka, Croatia

<sup>2</sup>Department of maritime sciences, University of Zadar, Mihovila Pavlinovića 1, 23000 Zadar, Croatia

E-mail: vedran.mrzljak@riteh.hr, jasna.prpic-orsic@riteh.hr, ipoljak1@unizd.hr, igospic@unizd.hr

**Abstract:** This paper presents thermodynamic (energy and exergy) analysis of backpressure (BPT) and condensing (CT) steam turbines from cogeneration system. Based on the measurement data from exploitation it is performed calculation of main operating parameters for both turbines and its comparison. Analysis shows that BPT develops significantly lower mechanical power (22821.90 kW) in comparison to CT (30893.10 kW), but also BPT has more than four times lower energy and exergy power losses when compared to CT. Due to much lower losses, BPT has significantly higher energy and exergy efficiencies (93.26% and 94.95%, respectively) in comparison to CT (82.63% and 83.87%, respectively). Energy and exergy power of a steam flow related to both observed turbines show that the BPT is the dominant heat supplier for all heat consumers inside the cogeneration system.

**KEYWORDS:** BACKPRESSURE STEAM TURBINE, CONDENSING STEAM TURBINE, THERMODYNAMIC ANALYSIS, COGENERATION SYSTEM

## 1. Introduction

Steam turbines, in a recent years, have a wide usage worldwide. The dominant function of a steam turbines is electrical power production in a various conventional or non-conventional steam power plants [1, 2]. However, steam turbines can also be found in a various marine propulsion systems [3-5], in a combined-cycle power plants (combined with gas turbines) [6, 7], as well as in various cogeneration systems where steam turbines are used for electrical power production and heat supply simultaneously [8].

Low-power steam turbines have an important role inside various plants or systems as an auxiliary components. Such steam turbines can be used also for the electrical power production [9, 10], for the drive of various high-pressure pumps [11, 12], or for the drive of various components which operation has an important role inside many plants or systems. Mentioned low-power steam turbines, in comparison to medium or high-power steam turbines, have a much lower efficiencies [13], but also various advantages and benefits in comparison to other power producers.

In the literature can be found various classifications of steam turbines [14]. One important classification is according to steam pressure at the turbine outlet – in this manner steam turbines are divided on backpressure and condensing steam turbines. Backpressure steam turbines have steam pressure at the outlet (after steam expansion inside the turbine) far above the atmospheric pressure – steam after such turbine is used for various heating purposes [15]. Steam pressure at the outlet of condensing steam turbines is far below the atmospheric pressure – such steam cannot be used anywhere else in the plant or system, it must be delivered to steam condenser for condensation [16].

This paper presents thermodynamic (energy and exergy) analysis of two steam turbines (backpressure and condensing) from cogeneration system. Based on the measured data from exploitation are calculated, presented and compared real (polytropic) and ideal (isentropic) mechanical power, energy and exergy power losses as well as the energy and exergy efficiencies of both analyzed turbines. The presented analysis gives an interesting comparison of backpressure and condensing steam turbines simultaneous operation.

## 2. Operating principle and description of the analyzed backpressure and condensing steam turbines

Scheme of the analyzed backpressure (BPT) and condensing (CT) steam turbines is presented in Fig. 1. In the same figure are clearly visible operating points where the measurements in exploitation are performed with an aim to obtain all the necessary steam operating parameters required for the analysis.

In the cogeneration system inside which the analyzed steam turbines operate, superheated steam is produced in steam generator [17] and delivered simultaneously to BPT and CT (with different mass flow rates). Both analyzed steam turbines have one steam

extraction – BPT through its extraction delivers a certain steam mass flow rate to the first heat consumer (Heat consumer 1), while CT through its extraction delivers a certain steam mass flow rate to the second heat consumer (Heat consumer 2). Steam after expansion in BPT is delivered to Heat consumer 2, while steam after expansion in CT has pressure significantly below the atmospheric one and can be delivered only to the steam condenser for condensation [18].

Along with satisfying the needs of both heat consumers (Heat consumer 1 and 2), both analyzed steam turbines produce electrical power by driving own electrical generators, Fig. 1.

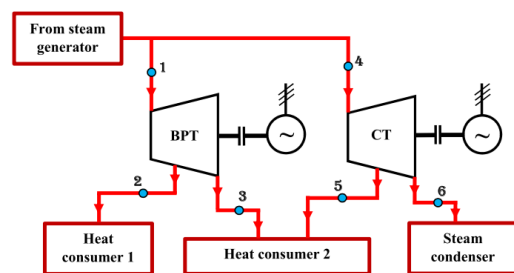


Fig. 1. Scheme of the analyzed backpressure (BPT) and condensing (CT) steam turbines from a cogeneration system

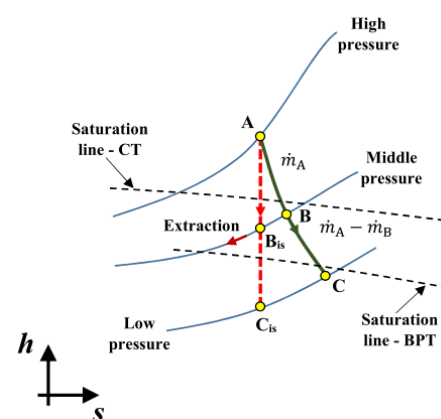


Fig. 2. General overview of real (polytropic) and ideal (isentropic) steam expansion processes inside BPT and CT in specific enthalpy-specific entropy diagram

Real (polytropic) and ideal (isentropic) steam expansion processes in specific enthalpy-specific entropy diagram of both analyzed steam turbines are presented in Fig. 2. Real (polytropic) steam expansion process is marked with green curve and operating points A-B-C. Ideal (isentropic) steam expansion process assumes always the same steam specific entropy during the expansion, this

process is in Fig. 2 marked with a red dashed line and operating points A-Bis-Cis. Ideal (isentropic) steam expansion process assumes the same steam mass flow rates and is performed between the same pressures as real (polytropic) steam expansion process.

For the BPT, operating points A-B-C from Fig. 2 corresponds to operating points 1-2-3 from Fig. 1. For the CT, points A-B-C from Fig. 2 corresponds to operating points 4-5-6 from Fig. 1.

### 3. Equations for thermodynamic analysis

#### 3.1. Overall equations for the energy and exergy analysis

Energy analysis of any system or a control volume has basis in the first law of thermodynamics [19, 20]. Overall energy balance equation, while disregarding potential and kinetic energies, can be written according to [21] as:

$$\dot{Q}_{IN} + P_{IN} + \sum \dot{E}n_{IN} = \dot{Q}_{OUT} + P_{OUT} + \sum \dot{E}n_{OUT}. \quad (1)$$

In Eq. 1 and throughout the paper, P is mechanical power in (kW), while  $\dot{Q}$  is energy heat transfer in (kW). Index IN corresponds to the system or component inlet (input) and index OUT corresponds to the system or component outlet (output).  $\dot{E}n$  is a total energy power of operating medium flow in (kW), defined according to [22] by following equation:

$$\dot{E}n = \dot{m} \cdot h. \quad (2)$$

In Eq. 2 and throughout the paper,  $\dot{m}$  is operating medium mass flow rate in (kg/s) and  $h$  is operating medium specific enthalpy in (kJ/kg). During system or a component operation usually did not occur operating medium mass flow rate leakage, so valid mass flow rate balance is [23]:

$$\sum \dot{m}_{IN} = \sum \dot{m}_{OUT}. \quad (3)$$

Exergy analysis of any system or a control volume has a basis in the second law of thermodynamics [24, 25]. The general exergy balance equation of any system or a control volume is defined as can be found in the literature [26] by using an equation:

$$\dot{X}_H + P_{IN} + \sum \dot{E}x_{IN} = P_{OUT} + \sum \dot{E}x_{OUT} + \dot{E}x_D. \quad (4)$$

In Eq. 4 and throughout the paper,  $\dot{E}x_D$  is exergy destruction (exergy power loss) in (kW), while  $\dot{X}_H$  is the exergy transfer by heat at the temperature  $T$  in (kW), defined by an equation [27]:

$$\dot{X}_H = \sum \left(1 - \frac{T_0}{T}\right) \cdot \dot{Q}. \quad (5)$$

In Eq. 5 and throughout the paper,  $T$  is temperature in (K), while index 0 corresponds to the ambient state.  $\dot{E}x$  is a total exergy power of operating medium flow in (kW) which can be calculated as [28]:

$$\dot{E}x = \dot{m} \cdot \varepsilon. \quad (6)$$

In Eq. 6 and throughout the paper,  $\varepsilon$  is specific exergy of operating medium in (kJ/kg), defined according to [29] by using an equation:

$$\varepsilon = (h - h_0) - T_0 \cdot (s - s_0). \quad (7)$$

In Eq. 7 and throughout the paper,  $s$  is specific entropy of operating medium in (kJ/kg·K). The general definition of any system or a control volume energy and exergy efficiency is:

$$\eta_{en,ex} = \frac{\text{cumulative energy (exergy) outlet (output)}}{\text{cumulative energy (exergy) inlet (input)}}. \quad (8)$$

Presented equations and balances will be used in energy and exergy analysis of both observed steam turbines (BPT and CT).

#### 3.2. Energy and exergy analysis equations of backpressure and condensing steam turbines

Equations for the energy and exergy analysis of backpressure (BPT) and condensing (CT) steam turbines are based on the operating points presented in Fig. 1. For the ideal (isentropic) steam expansion process are used the same operating points from Fig. 1

with abbreviation – is. All of the equations required for the BPT and CT analysis are presented in Table 1.

**Table 1.** Equations for the energy and exergy analysis of BPT and CT

Calculated parameter	BPT	Eq.	CT	Eq.
Real (polytropic) mechanical power	$P_{re,BPT} = \dot{m}_1 \cdot (h_1 - h_2) + (\dot{m}_1 - \dot{m}_2) \cdot (h_2 - h_3)$	(9)	$P_{re,CT} = \dot{m}_4 \cdot (h_4 - h_5) + (\dot{m}_4 - \dot{m}_5) \cdot (h_5 - h_6)$	(15)
Ideal (isentropic) mechanical power	$P_{is,BPT} = \dot{m}_1 \cdot (h_1 - h_{2is}) + (\dot{m}_1 - \dot{m}_2) \cdot (h_{2is} - h_{3is})$	(10)	$P_{is,CT} = \dot{m}_4 \cdot (h_4 - h_{5is}) + (\dot{m}_4 - \dot{m}_5) \cdot (h_{5is} - h_{6is})$	(16)
Energy power loss	$\dot{E}n_{L,BPT} = P_{is,BPT} - P_{re,BPT}$	(11)	$\dot{E}n_{L,CT} = P_{is,CT} - P_{re,CT}$	(17)
Energy efficiency	$\eta_{en,BPT} = \frac{P_{re,BPT}}{P_{is,BPT}}$	(12)	$\eta_{en,CT} = \frac{P_{re,CT}}{P_{is,CT}}$	(18)
Exergy destruction (exergy power loss)	$\dot{E}x_{D,BPT} = \dot{E}x_1 - \dot{E}x_2 - \dot{E}x_3 - P_{re,BPT}$	(13)	$\dot{E}x_{D,CT} = \dot{E}x_4 - \dot{E}x_5 - \dot{E}x_6 - P_{re,CT}$	(19)
Exergy efficiency	$\eta_{ex,BPT} = \frac{P_{re,BPT}}{\dot{E}x_1 - \dot{E}x_2 - \dot{E}x_3}$	(14)	$\eta_{ex,CT} = \frac{P_{re,CT}}{\dot{E}x_4 - \dot{E}x_5 - \dot{E}x_6}$	(20)

### 4. Steam operating parameters required for the energy and exergy analysis

Steam operating parameters (temperature, pressure and mass flow rate) in each operating point from Fig. 1 are found in [30] and presented in Table 2 for the real (polytropic) steam expansion process of both analyzed turbines (BPT and CT). Steam specific enthalpies, specific entropies and steam quality in each operating point from Fig. 1 are also presented in Table 2 – they are calculated by using NIST REFPROP 9.0 software [31]. Steam specific exergies in each operating point of each turbine presented in Table 2 are calculated for the ambient pressure of 1 bar and the ambient temperature of 25 °C by using Eq. 7.

**Table 2.** Steam parameters in each operating point of Fig. 1 – real (polytropic) expansion process

Turbine	Op. point*	Temp. (°C)	Pressure (bar)	Mass flow rate (kg/s)	Specific enthalpy (kJ/kg)	Specific entropy (kJ/kg·K)	Specific exergy (kJ/kg)	Steam quality
BPT	1	490.00	65.0	33	3393.2	6.8086	1367.80	Superh.
	2	210.00	8.0	5	2862.5	6.8653	820.20	Superh.
	3	127.41	2.5	28	2672.9	6.9435	607.21	0.98
CT	4	490.00	65.0	39	3393.2	6.8086	1367.80	Superh.
	5	127.41	2.5	25	2672.9	6.9435	607.21	0.98
	6	37.63	0.065	14	2472.8	7.9903	95.06	0.96

\* According to Fig. 1.

Steam operating parameters of the ideal (isentropic) expansion process required for the analysis are presented in Table 3.

**Table 3.** Steam parameters in each operating point of Fig. 1 – ideal (isentropic) expansion process

Turbine	Operating point**	Pressure (bar)	Mass flow rate (kg/s)	Specific entropy (kJ/kg·K)	Specific enthalpy (kJ/kg·K)
BPT	1	65.0	33	6.8086	3393.2
	2is	8.0	5	6.8086	2835.5
	3is	2.5	28	6.8086	2618.8
CT	4	65.0	39	6.8086	3393.2
	5is	2.5	25	6.8086	2618.8
	6is	0.065	14	6.8086	2105.6

\*\* According to Fig. 1 and Table 1.

### 5. Results and discussion

BPT real (polytropic) mechanical power is calculated by using Eq. 9, while the ideal (isentropic) mechanical power of the same turbine is calculated by using Eq. 10. In exploitation conditions, BPT shows a good performance because real (polytropic) mechanical power is only slightly lower in comparison to the ideal (isentropic) mechanical power (22821.90 kW in comparison to 24471.70 kW), Fig. 3.

Real (polytropic) and ideal (isentropic) mechanical power of a CT are calculated by using Eq. 15 and Eq. 16, respectively. Real (polytropic) steam expansion process of CT shows high difference in comparison to the ideal (isentropic) steam expansion process (real mechanical power is equal to 30893.10 kW, while ideal mechanical power is equal to 37386.40 kW), Fig. 3. Those results for CT leads to conclusion that the real expansion process can be significantly improved (with an aim to be as close as possible to the ideal one).

Direct comparison of BPT and CT from Fig. 3 leads to another conclusion that BPT produces significantly lower mechanical power (both ideal and real) in comparison to CT, but the real (polytropic) steam expansion process of BPT is much closer to the ideal (isentropic) one than in the case of CT. This element will result with much higher energy power loss of CT (in comparison to BPT).

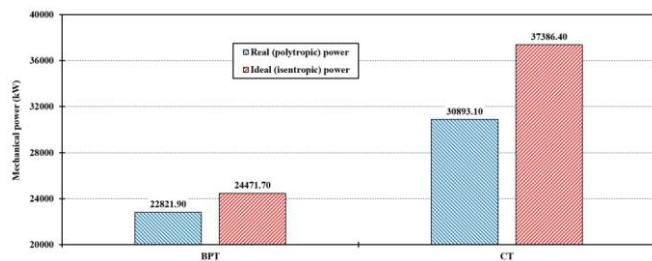


Fig. 3. Real (polytropic) and ideal (isentropic) mechanical power comparison of two analyzed steam turbines (BPT and CT)

A conclusion derived from Fig. 3 related to energy power loss of both observed steam turbines can be clearly seen in Fig. 4 – energy power loss of BPT is equal to 1649.80 kW, while energy power loss of CT is almost four times higher (6493.30 kW). Energy power loss of BPT is calculated by using Eq. 11, while energy power loss of CT is calculated by using Eq. 17.

The same trend related to energy power loss of both analyzed turbines is obtained in exergy power loss, with a note that CT has almost five times higher exergy power loss (exergy destruction) in comparison to BPT (5940.05 kW in comparison to 1212.62 kW), Fig. 4. Exergy power loss (exergy destruction) of BPT is calculated by using Eq. 13, while the same variable for CT is calculated by Eq. 19.

Therefore, for both analyzed turbines can be concluded that energy power loss and exergy power loss show the same trend and for both analyzed turbines exergy power loss (exergy destruction) is lower in comparison to the energy power loss.

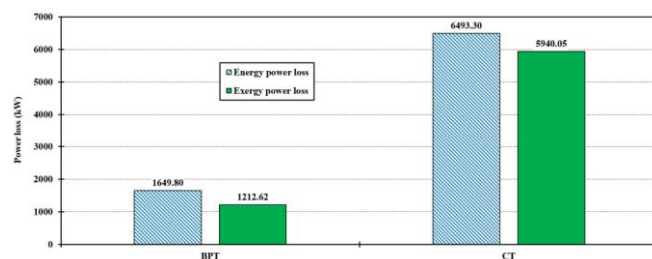


Fig. 4. Energy and exergy power loss of two analyzed steam turbines (BPT and CT)

Power loss and efficiency (energy or exergy) of various control volumes are usually reverse proportional. The same is valid for the observed steam turbines – BPT which has significantly lower power losses (energy or exergy) has significantly higher efficiencies

(energy or exergy) in comparison to CT, Fig. 4 and Fig. 5. Also, as for the both observed steam turbines exergy power loss (exergy destruction) is lower in comparison to the energy power loss, Fig. 4, exergy efficiencies of both observed steam turbines are higher than energy efficiencies, Fig. 5. For the BPT, obtained energy efficiency, calculated by using Eq. 12 is equal to 93.26%, while obtained exergy efficiency of the same turbine, calculated by using Eq. 14 is equal to 94.95%. For the CT, obtained energy efficiency, calculated by using Eq. 18 is equal to 82.63%, while obtained exergy efficiency of the same turbine, calculated by using Eq. 20 is equal to 83.87%, Fig. 5.

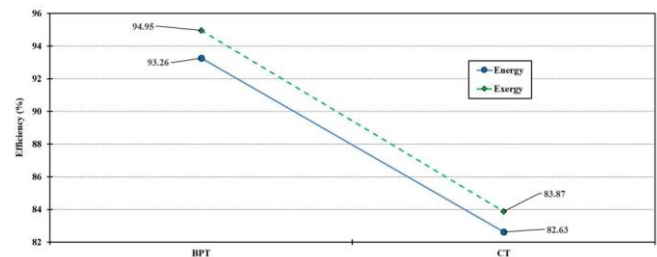


Fig. 5. Energy and exergy efficiency of two analyzed steam turbines (BPT and CT)

Energy and exergy power of each steam flow stream (in each operating point) from Fig. 1 are presented in Fig. 6. From Fig. 6 can also clearly be seen energy and exergy power of a steam flow delivered to all heat consumers. In each operating point from Fig. 1, energy power of a steam flow is calculated by using Eq. 2, while exergy power of a steam flow is calculated by using Eq. 6.

As expected, the highest energy and exergy power of a steam flow are related to inlet of both turbines (operating point 1 for BPT and operating point 4 for CT, Fig. 1). Due to higher steam mass flow rate delivered to CT inlet, both energy and exergy power of a steam flow are higher at the inlet of CT (in comparison to BPT inlet). Fig. 6 clearly presents that Heat consumer 1 is actually secondary heat consumer inside observed cogeneration system - energy and exergy power of a steam flow delivered to Heat consumer 1 are much lower in comparison to energy and exergy power of a steam flow delivered to Heat consumer 2 from each of the observed steam turbines. However, it should be noted that both energy and exergy power of a steam flow delivered to Heat consumer 2 are higher from BPT than from a CT. Therefore, BPT is more involved in satisfying Heat consumer 2 needs in comparison to CT.

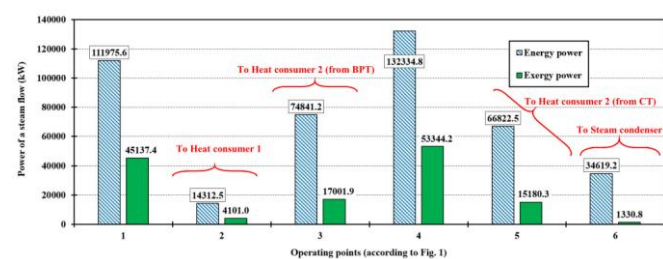


Fig. 6. Energy and exergy power of a steam flow in each operating point from Fig. 1.

From Fig. 6 can be also seen one expected fact – the lowest exergy power of a steam flow, while observing all operating points from Fig. 1, is related to steam flow delivered to Steam condenser (1330.8 kW). This fact can be explained from the exergy analysis definition – in comparison with energy analysis which did not take into account the conditions of the ambient in which control volume or a system operates, exergy analysis takes into account the temperature and pressure of the ambient in which control volume or a system operates. Steam flow which has a temperature the closest to the ambient temperature will have the lowest specific exergy, Table 2, and in this analysis that is a steam flow delivered to Steam condenser.

## 6. Conclusions

The paper presents thermodynamic (energy and exergy) analysis of backpressure (BPT) and condensing (CT) steam turbines from cogeneration system. Measured data from exploitation are used for calculation and comparison of real (polytropic) and ideal (isentropic) mechanical power, energy and exergy power losses as well as the energy and exergy efficiencies of both analyzed turbines. The most important conclusions from the performed analysis are:

- BPT in comparison to CT produces lower mechanical power (both real and ideal).
- Both power losses (energy and exergy) are significantly lower for BPT when compared to CT.
- Exergy power loss (exergy destruction) of both analyzed steam turbines is lower than energy power loss.
- Lower power losses of BPT results with significantly higher efficiencies (both energy and exergy) in comparison to CT.
- Energy and exergy power of a steam flow related to both observed turbines show that the dominant heat consumer inside the observed cogeneration system is Heat consumer 2.

## 7. Acknowledgment

This research has been supported by the Croatian Science Foundation under the project IP-2018-01-3739, CEEPUS network CIII-HR-0108, European Regional Development Fund under the grant KK.01.1.1.01.0009 (DATACROSS), project CEKOM under the grant KK.01.2.2.03.0004, CEI project "COVIDAI" (305.6019-20), University of Rijeka scientific grants: uniri-tehnic-18-275-1447, uniri-tehnic-18-18-1146 and uniri-tehnic-18-14.

## 8. References

[1] Ahmadi, G. R., Toghraie, D.: Energy and exergy analysis of Montazeri steam power plant in Iran, *Renewable and Sustainable Energy Reviews* 56, p. 454–463, 2016. (doi:10.1016/j.rser.2015.11.074)

[2] Erdem, H.H., Akkaya, A.V., Cetin, B., Dagdas, A., Sevilgen, S.H., Sahin, B., Teke, I., Gungor, C., Atas, S.: Comparative energetic and exergetic performance analyses for coal-fired thermal power plants in Turkey, *International Journal of Thermal Sciences* 48, p. 2179–2186, 2009. (doi:10.1016/j.ijthermalsci.2009.03.007)

[3] Mrzljak, V., Poljak, I.: Energy analysis of main propulsion steam turbine from conventional LNG carrier at three different loads, *International Journal of Maritime Science & Technology "Our Sea"* 66 (1), p. 10-18, 2019. (doi:10.17818/NM/2019/1.2)

[4] Koroglu, T., Sogut, O. S.: Conventional and advanced exergy analyses of a marine steam power plant, *Energy* 163, p. 392-403, 2018. (doi:10.1016/j.energy.2018.08.119)

[5] Mrzljak, V., Poljak, I., Prpić-Oršić, J.: Exergy analysis of the main propulsion steam turbine from marine propulsion plant, *Shipbuilding* 70 (1), p. 59-77, 2019. (doi:10.21278/brod70105)

[6] Ersayin, E., Ozgener, L.: Performance analysis of combined cycle power plants: A case study, *Renewable and Sustainable Energy Reviews* 43, p. 832–842, 2015. (doi:10.1016/j.rser.2014.11.082)

[7] Lorencin, I., Andelić, N., Mrzljak, V., Car, Z.: Genetic algorithm approach to design of multi-layer perceptron for combined cycle power plant electrical power output estimation, *Energies* 12 (22), 4352, 2019. (doi:10.3390/en12224352)

[8] Burin, E. K., Vogel, T., Multhaupt, S., Thelen, A., Oeljeklaus, G., Gorner, K., Bazzo, E.: Thermodynamic and economic evaluation of a solar aided sugarcane bagasse cogeneration power plant, *Energy* 117, Part 2, p. 416-428, 2016. (doi:10.1016/j.energy.2016.06.071)

[9] Behrendt, C., Stoyanov, R.: Operational characteristic of selected marine turbounits powered by steam from auxiliary oil-fired boilers, *New Trends in Production Engineering* 1 (1), p. 495-501, 2018. (doi:10.2478/ntp-2018-0061)

[10] Mrzljak, V., Senčić, T., Žarković, B.: Turbogenerator steam turbine variation in developed power: analysis of exergy efficiency and exergy destruction change, *Modelling and Simulation in Engineering* 2945325, 2018. (doi:10.1155/2018/2945325)

[11] Adibhatla, S., Kaushik, S. C.: Energy and exergy analysis of a super critical thermal power plant at various load conditions under constant and pure sliding pressure operation, *Applied Thermal Eng.* 73, p. 49-63, 2014. (doi:10.1016/j.applthermaleng.2014.07.030)

[12] Mrzljak, V., Prpić-Oršić, J., Poljak, I.: Energy power losses and efficiency of low power steam turbine for the main feed water pump drive in

the marine steam propulsion system, *Journal of Maritime & Transportation Sciences* 54 (1), p. 37-51, 2018. (doi:10.18048/2018.54.03)

[13] Mrzljak, V., Poljak, I., Mrakovčić, T.: Energy and exergy analysis of the turbo-generators and steam turbine for the main feed water pump drive on LNG carrier, *Energy Conv. and Management* 140, p. 307–323, 2017. (doi:10.1016/j.enconman.2017.03.007)

[14] Kostyuk, A., Frolov, V.: *Steam and gas turbines*, Mir Publishers, Moscow, 1988.

[15] Woodruff, E., Lammers, H., Lammers, T.: *Steam Plant Operation*, 8th edition, McGraw-Hill Professional, New York, USA, 2004.

[16] Aljundi, I.H.: Energy and exergy analysis of a steam power plant in Jordan, *Applied thermal engineering*, 29 (2-3), p.324-328, 2009. (doi:10.1016/j.applthermaleng.2008.02.029)

[17] Mrzljak, V., Poljak, I., Medica-Viola, V.: Dual fuel consumption and efficiency of marine steam generators for the propulsion of LNG carrier, *Applied Thermal Engineering* 119, p. 331–346, 2017. (doi:10.1016/j.applthermaleng.2017.03.078)

[18] Škopac, L., Medica-Viola, V., Mrzljak, V.: Selection Maps of Explicit Colebrook Approximations according to Calculation Time and Precision, *Heat Transfer Engineering* 42 (10), p. 839-853, 2021. (doi:10.1080/01457632.2020.1744248)

[19] Nandini, M., Sekhar, Y. R., Subramanyam, G.: Energy analysis and water conservation measures by water audit at thermal power stations, *Sustainable Water Resources Management* 7 (1), p. 1-24, 2021. (doi:10.1007/s40899-020-00487-4)

[20] Medica-Viola, V., Baressi Šegota, S., Mrzljak, V., Štifanić, D.: Comparison of conventional and heat balance based energy analyses of steam turbine, *Scientific Journal of Maritime Research* 34 (1), p.74-85, 2020. (doi:10.31217/p.34.1.9)

[21] Mrzljak, V., Prpić-Oršić, J., Senčić, T.: Change in steam generators main and auxiliary energy flow streams during the load increase of LNG carrier steam propulsion system, *Scientific Journal of Maritime Research* 32 (1), p. 121-131, 2018. (doi:10.31217/p.32.1.15)

[22] Mrzljak, V., Andelić, N., Poljak, I., Orović, J.: Thermodynamic analysis of marine steam power plant pressure reduction valves, *Journal of Maritime & Transportation Sciences* 56 (1), p. 9-30, 2019. (doi:10.18048/2019.56.01)

[23] Mrzljak, V., Poljak, I., Prpić-Oršić, J., Jelić, M.: Exergy analysis of marine waste heat recovery CO2 closed-cycle gas turbine system, *Scientific Journal of Maritime Research* 34 (2), p. 309-322, 2020. (doi:10.31217/p.34.2.12)

[24] Uysal, C., Kurt, H., Kwak H.-Y.: Exergetic and thermoeconomic analyses of a coal-fired power plant, *International Journal of Thermal Sciences* 117, p. 106-120, 2017. (doi:10.1016/j.ijthermalsci.2017.03.010)

[25] Naserbegi, A., Aghaie, M., Minucmehr, A., Alahyarizadeh, Gh.: A novel exergy optimization of Bushehr nuclear power plant by gravitational search algorithm (GSA), *Energy* 148, p. 373-385, 2018. (doi:10.1016/j.energy.2018.01.119)

[26] Mrzljak, V., Andelić, N., Lorencin, I., Baressi Šegota, S.: The influence of various optimization algorithms on nuclear power plant steam turbine exergy efficiency and destruction, *Scientific Journal of Maritime Research* 35 (1), p. 69-86, 2021. (doi:10.31217/p.35.1.8)

[27] Kowalczyk, T., Ziolkowski, P., Badur, J.: Exergy losses in the Szewalski binary vapor cycle, *Entropy* 17, p. 7242-7265, 2015. (doi:10.3390/e17107242)

[28] Elhelw, M., Al Dahma, K. S., Hamid Attia, A. E.: Utilizing exergy analysis in studying the performance of steam power plant at two different operation mode, *Applied Thermal Engineering* 150, p. 285–293, 2019. (doi:10.1016/j.applthermaleng.2019.01.003)

[29] Tan, H., Shan, S., Nie, Y., Zhao, Q.: A new boil-off gas re-liquefaction system for LNG carriers based on dual mixed refrigerant cycle, *Cryogenics* 92, p. 84–92, 2018. (doi:10.1016/j.cryogenics.2018.04.009)

[30] Kamate, S. C., Gangavati, P. B.: Energy and exergy analysis of a 44-MW bagasse-based cogeneration plant in India, *Cogeneration and Distributed Generation Journal* 25 (1), p. 35-51, 2010. (doi:10.1080/15453661009709861)

[31] Lemmon, E.W., Huber, M.L., McLinden, M.O.: *NIST reference fluid thermodynamic and transport properties-REFPROP*, version 9.0, User's guide, Colorado, 2010.